Journal of Energy in Southern Africa 19(1): 62–69
DOI: http://dx.doi.org/10.17159/2413-3051/2008/v19i1a3319

Electrical and thermal analysis of an asynchronous machine for application in wind energy generation

O I Okoro
University of Nigeria, Nsukka

E Chikuni
Polytechnic of Namibia, Windhoek, Namibia

Abstract
The electromagnetic (electrical) and mechanical design of an Asynchronous machine for application in wind energy generation depends on the knowledge of heat transfer within the various parts of the machine. Unfortunately, the analysis of thermal effect in Asynchronous motors is usually more complex, more non-linear and more difficult than the electromagnetic behaviour. This paper therefore, sets out to investigate the effect of coupling the electrical model with the thermal model of the machine. The results of the analysis show that the proposed coupled model is capable of predicting the stator phase currents, rotor bar temperature, stator windings temperature, heat losses, rotor speed and electromagnetic torque of the test machine under dynamic conditions and at rated load operation. The analysis finds application in wind energy generation especially when modified and applied to synchronous generators. By so doing, the prediction of critical temperatures of machine parts can be achieved prior to machine operation.

Keywords: asynchronous machine, electrical model, thermal model, coupling, wind energy, dynamic behaviour

1 Introduction

In many developing economies, the problem of frequent power outages and inadequate generating capacity, has made the call for a distributed generation imperative (Paalman & Morgan, 2005). Through this means electricity could be extended to remote villages that are not connected to the grid. Wind power has been noted to be a better alternative with worldwide wind energy capacity of 17.5GW at the end of 2000 pointing to its acceptability ((Paalman & Morgan, 2005; Momoh & Xu, 2005).

In recent times, induction machines have been used as a generator for a wind turbine system since it does not require any governor controls. It is also a very cost effective means of providing a generator for a turbine system with its almost fixed speed independent of torque variation capability compared to a synchronous machine. Wind turbine system include mechanical elements like shafts, gears or belts, which gear up or down the torque or speed of the motor and connect elements for mechanical power transmission for transformation of rotational into translatory motion. These elements show non-ideal transfer or dynamic characteristics making high precision speed and position control of the mechanical load extremely difficult (Okoro, 2003). Because of the nature of wind energy, it is important to keep track of the dynamics of the machine during operation. This means taking into account simultaneously both the mechanical and electrical behaviour of the machine to which the conventional model lacks. The dynamic behaviour of Asynchronous machines has received considerable attention in most researched works (Krause & Thomas, 1965; Okoro, 2002; Jordan, 1967).

In Krause & Thomas, (1965) the computer simulation of a symmetrical induction machine was carried out. Okoro (2002) investigated both the dynamic and thermal modelling of an induction machine with saturation and skin-effect included. In Jordan (1967), the digital computer simulation of induction machines in dynamic systems was discussed. In these papers no effort was made to investigate the effect of coupling the Electrical and Thermal models of the machine with the view of determining the overall machine behaviours in dynamic state.

Mellor et al (1995) and Griffith et al (1986) developed thermal models for an induction machine. Thermal networks, an equivalent of electrical networks are applied by Mellor *et al* (1995) while in Griffith *et al* (1986) the Finite-Element Method of analysis was used. Here again, the developed thermal models fail to take into account the me-

chanical and electrical models of the machine.

More recent work on Electrical-thermal coupling has been reported by Bastos et al (1997). The method used a weak coupled model in the analysis of the induction machine. This method of analysis has been noted to be computationally expensive in software development and hardware implementation since the Finite-Element Method was used in the analysis (Kylander, 1995).

This paper therefore looks at a simple method of modelling an Electrical-thermal coupled Asynchronous machine. The electrical model of the machine is first developed. Secondly, the mechanical model is presented. The paper continues with the development and analysis of the thermal model. Computer simulation and results with relevant conclusion conclude the paper. Figure 1 shows the proposed Electrical-Thermal Model of the Asynchronous machine.

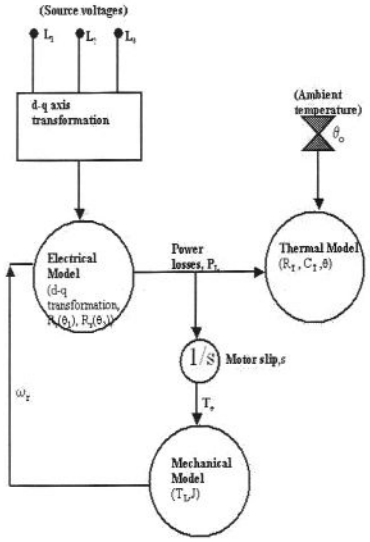

Figure 1: Block diagram of the proposed electrical-thermal model coupling

2 Electrical model

The non-linear differential equations which describe the dynamic performance of an ideal symmetrical Asynchronous machine in an arbitrary reference frame could be derived from the d-q equivalent circuits of Figure 2 as in (Krause & Thomas, 1965).

$$\begin{bmatrix} V_{qs} \\ V_{ds} \\ 0 \\ 0 \end{bmatrix} = \begin{bmatrix} (R_s + L_s p) & \omega L_s & L_m p & \omega L_m \\ -\omega L_s & (R_s + L_s p) & -\omega L_m & L_m p \\ L_m p & (\omega - \omega_r) L_m & (R_r + L_r p) & (\omega - \omega_r) L_r \\ -(\omega - \omega_r) L_m & L_m p & -(\omega - \omega_r) L_r & (R_r + L_r p) \end{bmatrix} \begin{bmatrix} i_{qs} \\ i_{ds} \\ i_{qr} \\ i_{dr} \end{bmatrix} \quad (1)$$

where,

$$L_s = L_{ls} + L_m \quad (2)$$

$$L_r = L_{lr} + L_m \quad (3)$$

$$p = \frac{d}{dt} \quad (4)$$

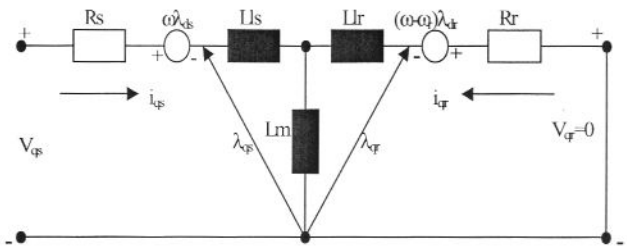

Figure 2a

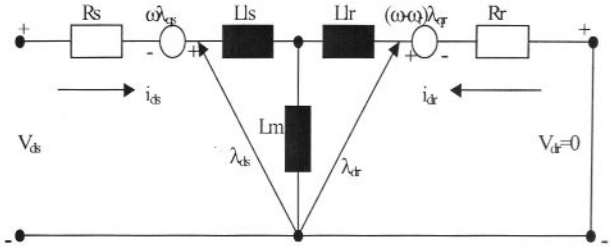

Figure 2b

Figure 2: Squirrel-cage asynchronous machine models in d-q axis: (a) q-axis model (b) d-axis model

Equation (1) can be transformed to d-q axis fixed on the rotor as in Levy et al (1990) by setting ω equal to ω_r. By so doing, equation (5) is the result.

$$\begin{bmatrix} V_{qs} \\ V_{ds} \\ 0 \\ 0 \end{bmatrix} = \begin{bmatrix} (R_s + L_s p) & \omega_r L_s & L_m p & \omega_r L_m \\ -\omega_r L_s & (R_s + L_s p) & -\omega_r L_m & L_m p \\ L_m p & 0 & (R_r + L_r p) & 0 \\ 0 & L_m p & 0 & (R_r + L_r p) \end{bmatrix} \begin{bmatrix} i_{qs} \\ i_{ds} \\ i_{qr} \\ i_{dr} \end{bmatrix} \quad (5)$$

For the purpose of digital simulation, equation (5) is represented in a state variable form with currents as state variables (Perdikaris, 1996).

$$p[\mathbf{i}] = -[\mathbf{L}]^{-1}([\mathbf{R}] + \omega_r[\mathbf{G}])[\mathbf{i}] + [\mathbf{L}]^{-1}[\mathbf{V}] \quad (6)$$

where,

$$[\mathbf{V}] = \begin{bmatrix} V_{qs} & V_{ds} & 0 & 0 \end{bmatrix}^t \quad (7)$$

$$[\mathbf{R}] = diag(R_s \quad R_s \quad R_r \quad R_r) \quad (8)$$

$$[\mathbf{L}] = \begin{bmatrix} L_s & 0 & L_m & 0 \\ 0 & L_s & 0 & L_m \\ L_m & 0 & L_r & 0 \\ 0 & L_m & 0 & L_r \end{bmatrix} \quad (9)$$

$$[\mathbf{G}] = \begin{bmatrix} 0 & L_s & 0 & L_m \\ -L_s & 0 & -L_m & 0 \\ 0 & 0 & 0 & 0 \\ 0 & 0 & 0 & 0 \end{bmatrix} \quad (10)$$

$$[\mathbf{i}] = \begin{bmatrix} i_{qs} & i_{ds} & i_{qr} & i_{dr} \end{bmatrix}^t \quad (11)$$

The Electromagnetic torque, Te is given by Krause (1986) as:

$$T_e = \frac{3}{2} P L_m \left(i_{qs} i_{dr} - i_{ds} i_{qr} \right) \quad (12)$$

where, P = Number of pole pairs.

Under a balanced condition, the stator voltages of a three-phase induction machine may be considered as sinusoidal and expressed as:

$$V_{as} = \sqrt{2} V \cos \omega_b t \quad (13)$$

$$V_{bs} = \sqrt{2} V \cos\left(\omega_b t - \frac{2\pi}{3} \right) \quad (14)$$

$$V_{cs} = \sqrt{2} V \cos\left(\omega_b t + \frac{2\pi}{3} \right) \quad (15)$$

These stator voltages are related to the d-q frame of reference by

$$\begin{bmatrix} V_{qs} \\ V_{ds} \end{bmatrix} = [C_1] \begin{bmatrix} V_{as} \\ V_{bs} \\ V_{cs} \end{bmatrix} \quad (16)$$

where,

$$[C_1] = \frac{2}{3} \begin{bmatrix} \cos\theta & \cos\left(\theta - \frac{2\pi}{3} \right) & \cos\left(\theta - \frac{4\pi}{3} \right) \\ \sin\theta & \sin\left(\theta - \frac{2\pi}{3} \right) & \sin\left(\theta - \frac{4\pi}{3} \right) \end{bmatrix} \quad (17)$$

Similarly, the stator phase currents are related to the d-q currents by

$$\begin{bmatrix} i_{as} \\ i_{bs} \\ i_{cs} \end{bmatrix} = [C]^{-1} \begin{bmatrix} i_{qs} \\ i_{ds} \\ i_0 \end{bmatrix} \quad (18)$$

$$[\mathbf{C}]^{-1} = \begin{bmatrix} \cos\theta & \sin\theta & 1 \\ \cos\left(\theta - \frac{2\pi}{3} \right) & \sin\left(\theta - \frac{2\pi}{3} \right) & 1 \\ \cos\left(\theta - -\frac{4\pi}{3} \right) & \sin\left(\theta - \frac{4\pi}{3} \right) & 1 \end{bmatrix} \quad (19)$$

3 Mechanical model

The mechanical model of an Asynchronous motor consists of the equations of motion of the motor and drive load as shown in Figure 3 and is usually represented as a second-order differential equation (Krause, 1986).

$$J_m p^2 \theta_m = T_e - T_L \quad (20)$$

Decomposing equation (20) into two first-order differential equations gives,

$$p\,\theta_m = \omega_m \quad (21)$$

$$J_m (p \omega_m) = (T_e - T_L) \quad (22)$$

But,

$$\omega_r = \omega_m P \quad (23)$$

$$\theta_r = \theta_m P \quad (24)$$

where,

ω_m = angular velocity of the rotor, θ_m = rotor angular position, θ_r = electrical rotor angular position, ω_r = electrical angular velocity, J_m= combined rotor and load inertia coefficient, T_L= applied load torque.

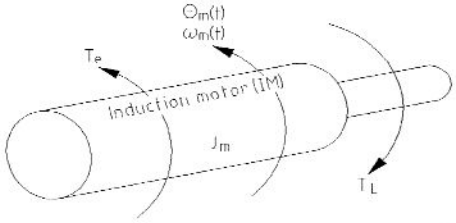

Figure 3: A schematic of a motor mechanical model

4 Thermal model

The thermal network model for the Squirrel-cage induction machine is developed according to the principles reported by Okoro (2002). The developed thermal network model is shown in Figure 4.

In this model, the stator iron and the frame constitute a network. The stator winding forms a separate network. The rotor iron and the copper components in the rotor are lumped into a network. The transient thermal network equations of the thermal model, taken node by node give:

$$\frac{d\theta_1}{dt} = \frac{1}{C_1} \left(P_1 - \frac{1}{R_{1a}} (\theta_1 - \theta_a) - \frac{1}{R_{12}} (\theta_1 - \theta_2) - \frac{1}{R_{13}} (\theta_1 - \theta_3) \right) \quad (25)$$

$$\frac{d\theta_2}{dt} = \frac{1}{C_2} \left(P_2 - \frac{1}{R_{24}} (\theta_2 - \theta_4) - \frac{1}{R_{21}} (\theta_2 - \theta_1) \right) \quad (26)$$

$$\frac{d\theta_3}{dt} = \frac{1}{C_3} \left(P_3 - \frac{1}{R_{31}} (\theta_3 - \theta_1) - \frac{1}{R_{34}} (\theta_3 - \theta_4) \right) \quad (27)$$

$$\frac{d\theta_4}{dt} = \frac{1}{C_4}\left(P_4 - \frac{1}{R_4}(\theta_{4b} - \theta_b) - \frac{1}{R_{42}}(\theta_4 - \theta_2) - \frac{1}{R_{43}}(\theta_4 - \theta_3)\right) \quad (28)$$

$P_1 \ldots P_2$ = heat losses in node1, node 2, etc, $\theta_1 \ldots \theta_2$ = temperature rises, $R_{1a} \ldots R_{43}$ = thermal resistances, $C_1 \ldots C_4$ = thermal capacitances.

The heat losses can be classified into ohmic and iron losses. The ohmic losses are load losses emanating from currents flowing through the stator and rotor windings. The ohmic losses of the stator and rotor are given mathematically by

$$P_{cu1} = 3R_s I_s^{\ 2} \quad (29)$$

$$P_{cu2} = 3R_r I_r^{\ 2} \quad (30)$$

The stator and rotor resistances are dependent on the motor temperature. Therefore, the measured resistance at room temperature (θ_0) must be corrected to a specified temperature (θ). The correction for the resistance change with temperature can be made by

$$R = R_{20}\frac{K + \theta}{K + \theta_0} \quad (31)$$

Where R is the corrected resistance at θ, and K is equal to 245 for Aluminium and 235 for Copper.

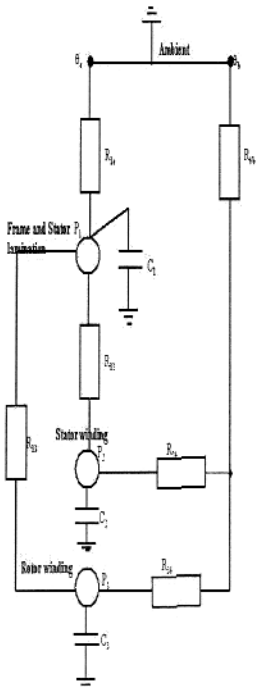

Figure 4: Simplified thermal network model

The iron losses consist of the eddy current losses and hysteresis losses. The empirical form of these losses is given by Klamt (1962) as:

$$P_H = \sigma_H \frac{f}{100} B^2 m \quad (32)$$

$$P_E = \sigma_E \left(\Delta_{Fe}\frac{f}{100} B\right)^2 m \quad (33)$$

$$P_{Fe} = P_H + P_E = \left[\sigma_H \frac{100}{f} + \sigma_E \Delta_{Fe}^{\ 2}\right]\left(\frac{f}{100}\right)^2 B^2 m \quad (34)$$

where,

σ_H = Hysteresis loss Coefficient,

σ_E = Eddy-current loss Coefficient,

Δ_{Fe} = the thickness of the lamination sheet, m = mass, f = frequency, B = magnetic flux density.

5 Coupling of electrical and thermal models

The interaction of the electrical, mechanical and thermal models is realised by coupling the electrical model with the thermal model as shown in Figure 1. The Electrical model is expected to determine the losses dissipated in the various parts of the rotor. The stator and rotor equivalent resistances are varied as functions of their average temperatures. The thermal model is derived by considering the power losses and rate of temperature rise in various parts of the motor. The model thermal resistances and capacitances are evaluated using the motor construction data. The input to the thermal model is calculated from the electrical model. The mechanical model consists of the equations of motion of the motor and driven load.

By using the mechanical model, motor speed can be measured or calculated during motor operation. The mechanical model, therefore presents the motor speed as an input to the electrical model. Therefore, by coupling the electrical and thermal models, the power losses of the thermal model are given by the electrical model while the temperatures in the equivalent resistances used in the electrical model are corrected by the thermal model.

The two models are calculated in parallel. It is imperative to state that before each calculation step of temperatures, the heat loss inputs have to be determined. The strategy for evaluating these losses for every need of the thermal model takes enormous computer time -- since the thermal time constants of the motor are higher than the electrical ones. In order to reduce the simulation time as well as the transient time, the calculated thermal time constants of the motor are further reduced by a factor of 100. The mathematical representation of the coupled system in state variable form is,

$$\left[\dot{\mathbf{x}}\right] = \left[\dot{i} \quad \dot{\omega}_r \quad \dot{\theta}_r \quad \dot{\theta}_{ih}\right]^t \quad (35)$$

The first variable in equation (35) represents the electrical model. The second and third terms represent the mechanical model, while the last term connotes the thermal model.

6 Experimentation and simulation results

The test machine is a Schorch VDE 0530, class F insulation, surface cooled squirrel-cage asynchronous motor as shown in Figure 5. The rated power, speed and current are 4.8 KW, 1 465 rpm and 18.5 A respectively. The test machine is a four-pole motor with 50 Hz rated frequency and 180 V rated voltage.

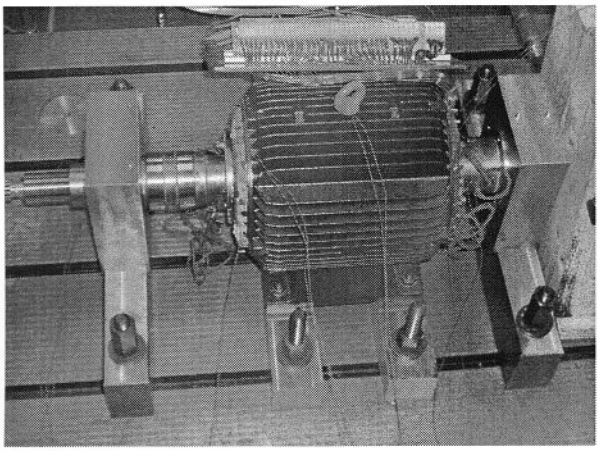

Figure 5: The 4.8KW squirrel-cage induction motor

Several tests were carried out on the test machine in order to determine the electrical and mechanical quantities of the machine (Okoro, 2002). The results of these tests together with the name plate parameters of the motor are shown in Table 1.

Table 1: Test machine parameters

Rated frequency	50Hz
Rated voltage (Delta connection)	180V
Rated current	18.5A
Number of poles	4
Mechanical load torque	31Nm
Rated power	4.8KW
Rotor resistance	0.53Ω
Stator resistance	0.60Ω
Stator leakage inductance	1.87mΩ
Rotor leakage inductance	5.73mΩ
Magnetizing inductance	0.48Ω
Estimated rotor inertia moment	0.0303821kgm^2

The values of the thermal resistances and capacitances were calculated according to the principles reported by Okoro (2002). Table 2 shows the computed values.

Table 2: Calculated thermal resistances and capacitances

Thermal capacitances	*Values (J/K)*	*Thermal resistances*	*Values (K/W)*
C1	22897.175	R_{1a}	0.0416
C2	963.308	R_{4b}	0.015
C3	3831.132	R_{12}	10.749 X 10^{-3}
		R_{24}	0.16022
C4	1006	R_{13}	0.092
		R_{34}	0.0948

The developed electrical-thermal model gives rise to a set of differential equations which describe both the thermal and electromechanical behaviours of the machine under dynamic conditions. MATLAB m-files were developed in other to determine the average temperature rise in the various parts of the machine as well as losses in the machine (MATLAB, 1991). The MATLAB m-files use the Runge-Kutta numerical method (Gerald, 1978) to solve the state variable representation of proposed electrical-thermal model as indicated in equation (35).

The time function of the speed, electromagnetic torque, stator phase currents and resistances is depicted in Figures 6 – 8. Figures 9 and 10 show the heat losses associated with the component parts of the test machine. The graph of rotor speed as against time in Figure 6 shows that the speed of the machine drops at time equals 0.5s due to load applications. But at the instant of the load application, the torque increases from 0Nm to 31Nm which is the value of the mechanical load torque as the electromagnetic-time curve of Figure 6 depicts.

Figure 7 shows that the transient period of the machine dies down about 0.15s after start-up. However, the magnitude of the steady state value of the stator phase currents increases as the load is applied at time equals 0.5s. Figure 8 shows that both the stator and rotor resistances have an initial peak rise but remain constant after the application of load. Figures 9 and 10 show that great amount of heat losses occur at the rotor iron and rotor bar of the test machine. The stator iron and frame have the least heat losses as Figure 10 indicates.

Figure 11 shows the temperature rise of the various parts of the machine. The rotor iron and rotor bar respond sharply to heat compared to other parts of the machine with a peak temperature of about 125^{0}C.

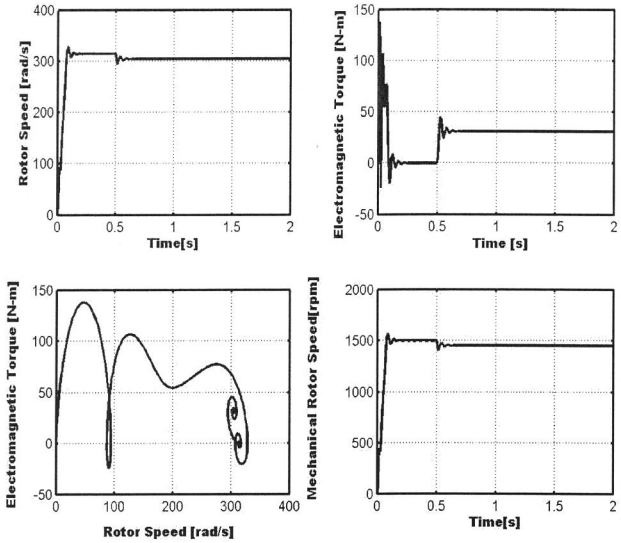

Figure 6: Predicted time function of speed and torque at run-up condition

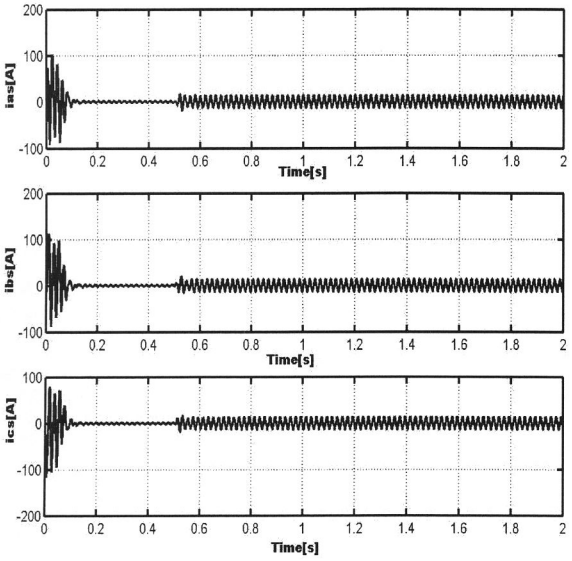

Figure 7: Predicted time function of stator phase currents at run-up condition

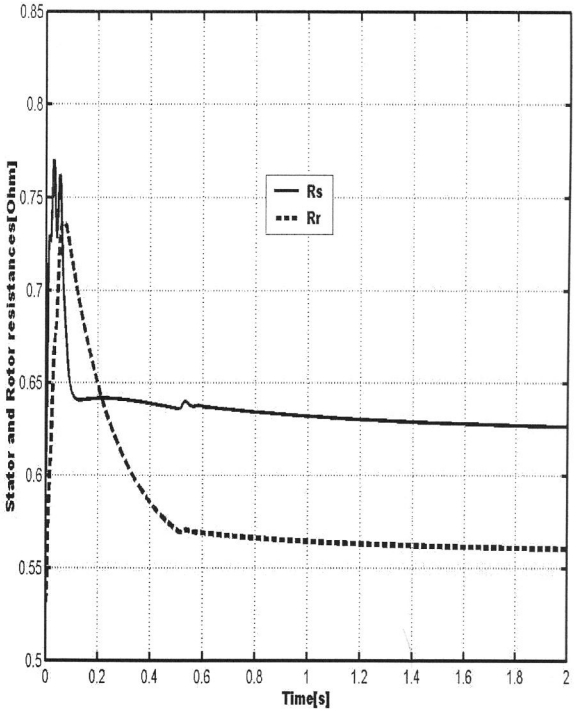

Figure 8: Predicted time function of stator and rotor resistances

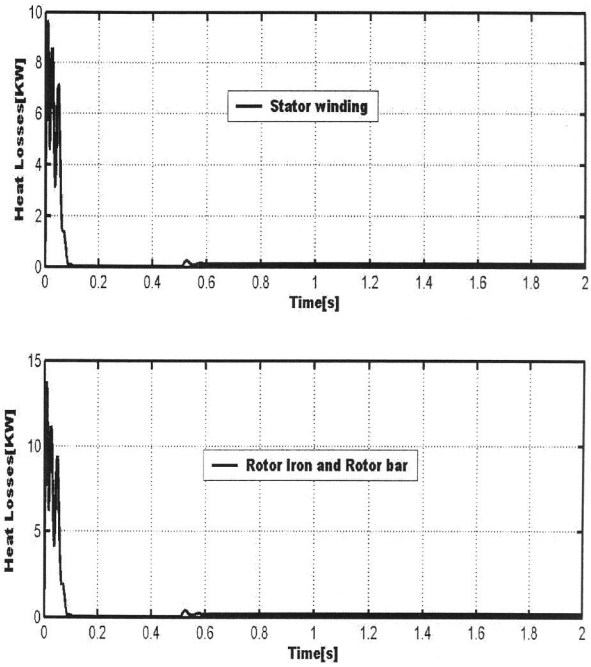

Figure 9: Predicted time function of heat losses in stator winding and rotor iron and bar

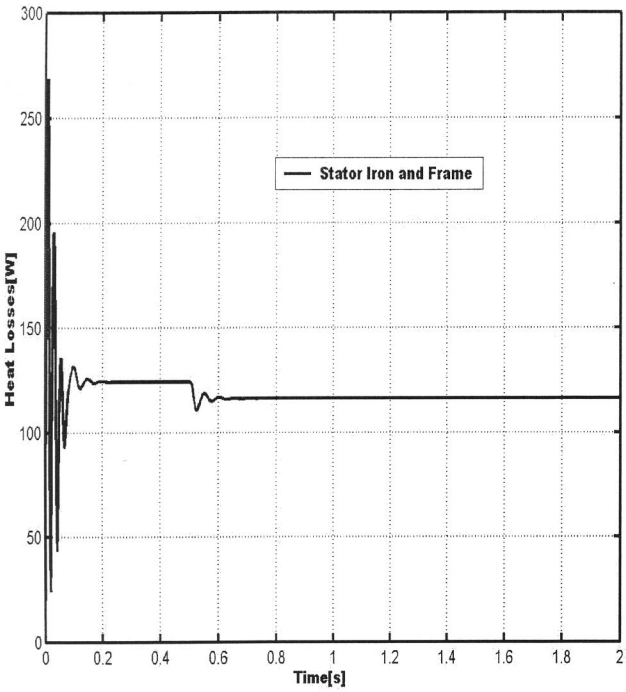

Figure 10: Predicted time function of heat losses in stator iron and frame

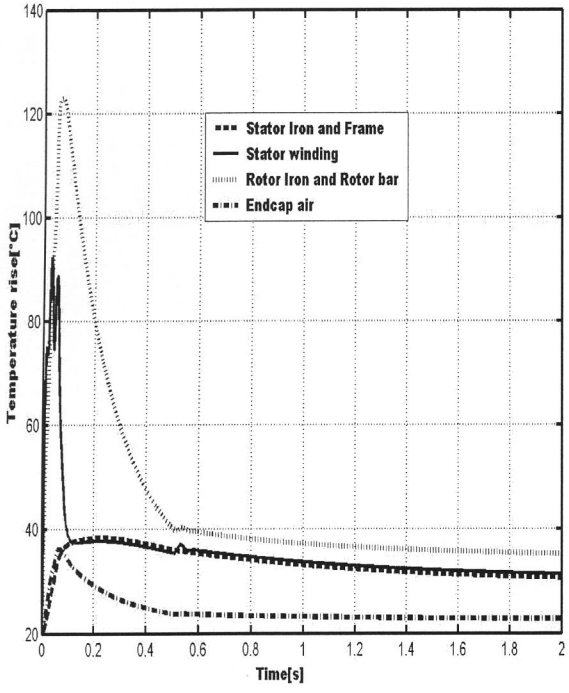

Figure 11: Predicted temperatures of the coupled models

7 Conclusion

The electrical, mechanical and thermal interactions in an Asynchronous motor have been presented in this paper by coupling an electrical model with a thermal model. A d-q axis model has been used to predict the electrical characteristics of the machine with temperature effect and heat losses incorporated. The developed thermal model parameters can be determined easily from dimensional information, the thermal properties of the materials used in designing the machine and the constant heat transfer coefficients.

The analysis presented in this paper is useful when the motor is fed by a PWM inverter and is expected to operate under variable load conditions as in the case of wind energy generation. Thus, the temperature rises of the various machine parts as a result of load variations can easily be predicted.

Nomenclature

R_s	Stator resistance (Ω)
I_s	Stator current per phase (A)
R_r	Rotor resistance (Ω)
I_r	Rotor current per phase (A)
L_m	Magnetizing inductance (H)
L_s	Stator self inductance (H)
L_r	Rotor self inductance (H)
L_{ls}	Stator leakage inductance (H)
L_{lr}	Rotor leakage inductance (H)
PWM	Pulse width modulation
ω_r	Rotor angular speed (rad/s)
ω_s	Synchronous speed (rad/s)
i_{qs}	q-axis stator current (A)
i_{ds}	d-axis stator current (A)
i_{qr}	q-axis rotor current (A)
i_{dr}	d-axis rotor current (A)
V_{ds}	d-axis stator voltage (V)
V_{qs}	q-axis stator voltage (V)
J_m	Motor inertia moment (Kgm^2)

Acknowledgement

The first author wishes to thank Prof. Dr.-Ing. B. Weidemann for his useful discussion on the subject and to DAAD for their financial assistance during the research work at the University of Kassel, Germany.

References

Bastos, J.P; Cabriera, M.F.R.R; Sadowski, N and Arruda, S.R.: 'A thermal analysis of induction motors using a weak coupled modelling', IEEE Transactions on Magnetics, Vol. 33 No. 2, March 1997, pp. 1714-1717.

Gerald, C.F.: *Applied Numerical Analysis*, Addison-Wesley publishing company, London, 1978.

Griffith, J.W; McCoy, R.M and Sharma, D.K: 'Induction motor squirrel cage rotor winding thermal analysis', IEEE Transactions on Energy Conversion, Vol. EC-1 No.3, September 1986, pp. 22-25.

Jordan, H.E: 'Digital computer analysis of induction machines in dynamic systems', IEEE Transactions on Power Apparatus and Systems, Vol. PAS-86 No.6, June 1967, pp.722-728.

Klamt, J.: Berechnung und Bemessung elektrischer Maschinen, Springer Verlag, 1962.

Krause P.C and Thomas C.H: 'Simulation of symmetrical induction machinery'; Transactions IEEE, Vol. PAS-84 No. 11, 1965, pp. 1038-1053.

Krause, P.C.: *Analysis of Electric Machinery*, New York, McGraw-Hill, 1986.

Kylander, G: *Thermal modelling of small cage induction motors*, Doctor of Technology Thesis, Chalmers University of Technology, Gothenburg, Sweden, 1995.

Levy, W; Landy, C.F. and McCulloch, M.D.: 'Improved models for the simulation of deep bar induction motors', IEEE Transactions on Energy Conversion, Vol. 5 No. 2, June 1990, pp. 393-400.

Mellor, P.H; Roberts, D and Turner, D.R; 'Lumped parameter thermal model for electrical machines of TEFC design', IEE proc. B Vol. 135 No. 5, 1995, pp.205-218.

Momoh, J.A. and Xu, Kaili: 'Evaluation of Renewable energy options for national electricity needs', Proceedings of the 6th International conference on power systems operation and planning, 22-26 May 2005, pp. 13-21.

Okoro O.I: Dynamic and thermal modelling of induction machine with non-linear effects, Kassel University Press, Kassel, September 2002.

Okoro, O.I.: 'Computer Simulation of Induction Machine coupled to a mechanical load', Nigerian Journal of Engineering Management, Vol. 4 No. 4, 2003, pp. 28-38.

Paalman, E. and Morgan, R.: 'Electricity supply to a remote village using grid-connected wind generators', Proceedings of the 13th conference on the Domestic Use of Energy, 29-31 March 2005, pp.131-136.

Perdikaris, G.A.: *Computer Controlled systems: Theory and Applications,* Kluwer Academic Publishers, Netherlands, 1996.

The MATLAB User's guide, The Mathworks Inc, Natick, 1991.

Received 26 April 2007, revised 31 January 2008